

# Investigating two- $\gamma$ -phonon vibrational states in $^{162}\text{Dy}$ through Coulomb excitation

Thomas Perissinotto<sup>1,\*</sup>, A. J. Mitchell<sup>1,\*\*</sup>, Ben Coombes<sup>1</sup>, Jack Woodside<sup>1</sup>, Claes Fahlander<sup>2</sup>, Andrew Stuchbery<sup>1</sup>, Gregory Lane<sup>1</sup>, Aditya Babu<sup>1</sup>, Hanaa Alshammari<sup>3</sup>, Victoria Bashu<sup>1</sup>, Ferdos Dastgiri<sup>1,\*\*\*</sup>, Rikako Kono<sup>1</sup>, and Lachlan McKie<sup>1</sup>

<sup>1</sup>Department of Nuclear Physics and Accelerator Applications, Research School of Physics, The Australian National University, Canberra, ACT 2601, Australia.

<sup>2</sup>Department of Physics, Lund University, 22100 Lund, Sweden

<sup>3</sup>Department of Physics, College of Science, Northern Border University, Arar, Saudi Arabia.

**Abstract.** The existence of two- $\gamma$ -phonon excited states in rare-earth nuclei remains a contentious issue in nuclear structure. While examples of single-phonon  $\gamma$ -vibrational states are prevalent in even-even deformed nuclei, identifying two-phonon excitations is challenging due to strength fragmentation and competing non-collective states. Although states with a strong two-phonon contribution are predicted by the collective model of Bohr and Mottelson, experimental evidence remains scarce, with only six cases reported in rare-earth nuclei. While properties of these states are largely in agreement with predictions from the model, their rarity challenges its validity. This work presents an overview of a Coulomb-excitation investigation into the low-lying states of  $^{162}\text{Dy}$ , which exhibits two  $K^\pi = 4^+$  states suspected to be a splitting of the two- $\gamma$ -phonon contribution. Analysis methods for determining reduced transition matrix elements  $\langle I_f || E_\lambda || I_i \rangle$ , a key indication of collectivity, are presented. A new particle-detector array under development to enhance the Coulomb-excitation capabilities at the Australian Heavy Ion Accelerator Facility is also discussed.

## 1 Introduction

The discrete nature of nuclear excitations has been observed for over a century, primarily through the detection of characteristic  $\gamma$  rays emitted during the de-excitation process. However, the nuclear-structure models developed to explain these excitation and de-excitation processes often fail to reproduce experimental observations.

In particular, two- $\gamma$ -phonon vibrational excitations, a prediction of the Bohr collective model [1], are rare throughout the rare-earth nuclei despite the prevalence of single- $\gamma$  excitations across the region. Therefore, the exact nature of the proposed two- $\gamma$ -phonon states (a  $K^\pi = 4^+$  state in  $^{168}\text{Er}$  [2, 3],  $K^\pi = 4^+$  and  $0^+$  states in  $^{166}\text{Er}$  [4], a  $K^\pi = 4^+$  state in  $^{164}\text{Dy}$  [5], and two  $K^\pi = 4^+$  states in  $^{162}\text{Dy}$  [6]) is called into question. Simply put: if these truly are two-phonon excitations, why are these the only observed cases? Or alternatively, if these are not two-phonon excitations, what are they and what consequences does this have for the vibrational model?

### 1.1 Vibrational excitations in nuclei

In deformed and near-spherical nuclei, band-head excitations at low energy can often be described in terms of quantised surface vibrations of the nuclear shape [1].

In the quantum-mechanical picture, vibrational excitations are mediated by phonons, bosonic quasiparticles representing coherent superpositions of particle-hole excitations across the Fermi surface. While this harmonic-oscillator-based model does not predict the energy of quadrupole phonons, it does require that they have an angular momentum of  $2\hbar$  and even parity, such that the first band-head state with spin-parity  $2^+$  is often attributed to a single-quadrupole-phonon excitation. This assignment is aided by the fact that monopole and dipole modes are suppressed at energies below 20 MeV [7].

In nuclei with a deformed ground state (such as  $^{162}\text{Dy}$ ), quadrupole vibrations can be further classified according to the symmetry of the deformation: so-called  $\beta$  vibrations correspond to oscillations that preserve axial symmetry, while  $\gamma$  vibrations break it.

### 1.2 Two-phonon excitations

When multiple vibrational quanta are excited simultaneously, the resulting states can be interpreted as coupled-phonon systems. In the case of  $\gamma$  vibrations, each one-phonon excitation carries a projection  $K = 2$  of the angular momentum onto the symmetry axis. When two such phonons are coupled, the possible projections are  $K = 0, 2, 4$ . However, symmetry constraints restrict the possible combinations to  $K = 0$  and  $K = 4$ ; the antisymmetric  $K = 2$  component vanishes [8].

In the ideal harmonic limit, the excitation energy of these two-phonon bands is expected to be exactly twice that of

\*e-mail: tom.perissinotto@anu.edu.au

\*\*e-mail: aj.mitchell@anu.edu.au

\*\*\*Current address: Department of Physics and Astronomy, University College London, London WC1E 6BT, United Kingdom.

the one-phonon bandhead,  $E_{2\text{-phonon}} = 2E_{1\text{-phonon}}$ . However, in practice, deviations from ideal ratios are expected. Anharmonicity in the potential, configuration mixing, and coupling to rotational motion can fragment the two-phonon strength across multiple states, making experimental identification challenging. A characteristic signature remains the  $B(E2)$  transition strength from the two-phonon states to the one-phonon band compared to transitions directly to the ground state, reflecting the underlying phonon-coupling algebra.

### 1.3 Dysprosium-162

Figure 1 shows a partial level scheme of  $^{162}\text{Dy}$ , a rare-earth, even-even nucleus with a well-deformed prolate ground state and a rich set of low-lying collective excitations. Of primary interest for the present study is the  $K^\pi = 2^+$  band-head at 888 keV, which is widely accepted as the single- $\gamma$ -phonon excitation, and similarly identified states are common across many rare-earth nuclei.

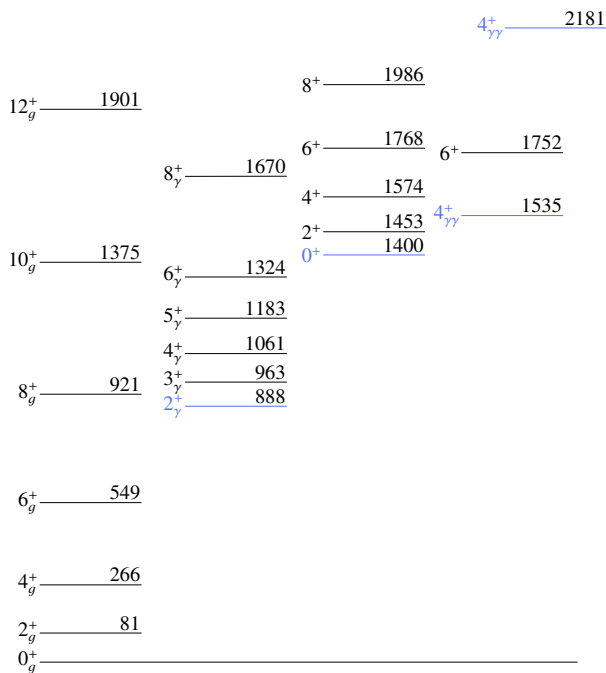


Figure 1: Partial level scheme of  $^{162}\text{Dy}$  with energies given in keV, based on evaluated nuclear data sheets [9]. The collective band-head states discussed in the text are highlighted in blue.

Two distinct  $K^\pi = 4^+$  bands are observed at 1535 keV and 2181 keV. Both of these  $4^+$  bands have been discussed in the literature as containing a two- $\gamma$ -phonon contribution. This circumstance is notable: it represents the only documented case in which two-phonon contributions appear split between states with the same spin, and it raises questions about the role of anharmonicity and configuration mixing in distributing two-phonon strength among nearby states [6, 10].

In addition to the two  $4^+$  bands, the lowest non-yrast  $0^+$  band in  $^{162}\text{Dy}$  has a complicated history of interpreta-

tion. Early spectroscopy identified this level as a candidate for  $\beta$ -vibration [10]; however, more recent lifetime and branching-ratio measurements have revealed a comparatively strong transition to the single- $\gamma$ -phonon band, suggesting significant mixing with  $\gamma$ -vibrational configurations or alternative structural interpretations [11]. Heyde and Wood suggest shape coexistence as a contributing factor in all low-lying excited  $0^+$  states, and in particular point to the smaller energy-spacing in this band as an example [12]. This all underscores the need for additional, high-precision measurements of transition strengths to disentangle the competing configurations.

### 1.4 Aim

In this proceedings, we report on experimental work undertaken at the Australian National University to investigate the low-lying ( $\leq 2$  MeV) excited states in  $^{162}\text{Dy}$  through Coulomb excitation. This includes an overview of how experimental particle-gated  $\gamma$ -ray energy spectra were converted into  $\gamma$ -ray yields and the Gosia minimisation process required to determine transition strengths.  $B(E2)$  transition strengths are a key indication of collectivity and two-phonon contributions, and so accurate measurements across the whole level scheme are required.

Preliminary results are briefly discussed; however, more work is required before final conclusions can be drawn. A discussion of the future direction of the investigation, including the development of a new particle detection array for increased Coulomb excitation capabilities, is also presented.

## 2 Coulomb Excitation

Coulomb excitation is a well-established technique for studying the collective properties of nuclei, schematically represented in Fig. 2. In this process, a projectile nucleus (in this case,  $^{16}\text{O}$ ) is directed at a target nucleus ( $^{162}\text{Dy}$ ) with a beam energy below the Coulomb barrier, ensuring that the interaction is purely electromagnetic and that no nucleon transfer or fusion occurs. The criteria to ensure  $\leq 0.1\%$  influence of unwanted scattering channels is given by

$$E_{Max} = 1.44 \frac{A_1 + A_2}{A_2} \cdot \frac{Z_1 Z_2}{1.25(A_1^{1/3} + A_2^{1/3}) + 5} \text{ MeV}, \quad (1)$$

where  $Z_1, A_1$  and  $Z_2, A_2$  refer to the beam and target nuclei respectively [13].

The time-dependent electric field of one nucleus acts to excite collective states in the other, with the probability of excitation determined by the strength and multipolarity of the electromagnetic interaction. Since the Coulomb force is well understood, the excitation process can be modelled using semiclassical or fully quantum-mechanical formalisms, allowing the determination of transition strengths and electric quadrupole moments from the measured  $\gamma$ -ray yields.

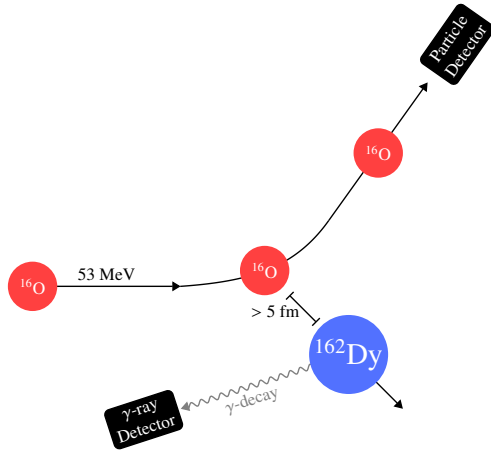


Figure 2: Schematic representation of Coulomb excitation. A projectile nucleus (red) interacts electromagnetically with a target nucleus (blue) at an impact parameter large enough to avoid nuclear contact. The resulting  $\gamma$  rays are detected in coincidence with scattered beam particles.

## 2.1 Experimental details

The investigation into low-lying states of  $^{162}\text{Dy}$  was undertaken at the Heavy Ion Accelerator Facility (HIAF) [14] in April, 2024. Using the 14UD Pelletron accelerator, a beam of  $^{16}\text{O}$  ions with an intensity of  $\approx 4$  pA was accelerated to 53 MeV, which represents 95% of Cline’s safe-energy criterion (Eqn. 1). The beam was incident on a  $1.5 \text{ mg} \cdot \text{cm}^{-2}$  self-supporting  $^{162}\text{Dy}$  target with an isotopic enrichment of 96.26%.

The Compton-suppressed array (CAESAR) was used to detect de-excitation  $\gamma$  rays and back-scattered beam particles. CAESAR consists of a target chamber designed to accommodate ancillary particle detectors around a retractable target ladder, surrounded by nine high-purity germanium (HPGe)  $\gamma$ -ray detectors arranged with six in the vertical plane and three in the horizontal plane. Compton-scattering events were suppressed via bismuth germinate (BGO) detectors surrounding each HPGe detector, themselves shielded by lead collimators.

The particle-detector array inside the target chamber consisted of eight rectangular silicon photodiodes (SiPD) positioned approximately symmetrically about the beam axis at backwards angles in the horizontal plane. The array covers polar scattering angles in the range  $[58^\circ, -60^\circ]$ , and is identical to the  $^{16}\text{O}$  array described in more detail in Ref. [15].

## 3 Preliminary Analysis

### 3.1 Experimental $\gamma$ -ray yields

An XIA Pixie-16 digital data acquisition system was used to record preamplified signals from HPGe detectors, their BGO suppressors, and the silicon photodiodes. These signals were time-stamped, and using a coincidence window

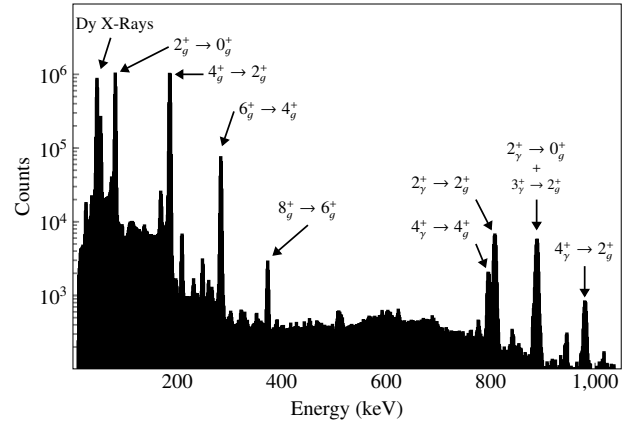


Figure 3: Summed particle- $\gamma$  coincidence  $\gamma$ -ray energy spectrum. Peaks corresponding to transitions between even-parity states of  $^{162}\text{Dy}$  are labelled, in accordance with Fig. 1.

of 3  $\mu\text{s}$ , coincidence events were constructed. The particle- $\gamma$  time-difference spectrum showed a clear peak with a width of 500 ns, so a timing cut around this peak was applied with random background subtractions from both sides.

Additional software energy gates set on the particle spectra were used to isolate  $^{16}\text{O}$ -Dy scattering events from low-mass particles (such as electrons) as well as  $^{16}\text{O}$  scattering off a surface contaminant, identified as  $^{232}\text{Th}$ . It is noted that  $^{16}\text{O}$  ions scattered off other isotopes of Dy, present in the target at a few percent level, could not be distinguished using the particle detectors.

The total particle-gated, Doppler-corrected  $\gamma$ -ray energy spectrum is shown in Fig. 3. Unlabelled peaks correspond to odd-parity transitions in  $^{162}\text{Dy}$ , as well as transitions in other Dy isotopes.

Using a sum-over-background method to account for the low-energy tail of the roughly Gaussian peaks, peak-area measurements were then corrected for detector efficiencies and angular correlations to produce total  $\gamma$ -ray yields (Table 1) in coincidence with each particle detector according to

$$Y_{\text{Exp}} = C \left\{ \sum_i \eta_{\text{abs}}(E_{\gamma,i}) W(\theta_{\gamma,i}, \Delta\phi_i) \right\}^{-1}, \quad (2)$$

where  $C$  is the measured peak area,  $\eta_{\text{abs}}(E_{\gamma,i})$  is the absolute efficiency of HPGe detector  $i$ , and  $W(\theta_{\gamma,i}, \Delta\phi_i)$  accounts for the angular correlation between particle and  $\gamma$ -ray detectors. The solid-angle coverage of the HPGe detectors was also accounted for, to produce an experimental  $4\pi$   $\gamma$ -ray yield which was then input into the Gosia code.

### 3.2 Transition strengths through Gosia minimisation

Gosia is a numerical code based on the semi-classical theory of Coulomb excitation [16]. Through least-squares

Table 1: Experimental  $\gamma$ -ray yields ( $Y_{\text{corr}}$ ) for observed transitions in  $^{162}\text{Dy}$ , summed over all particle detectors. States are labelled in accordance with Fig. 1.

Transition	Energy (keV)	$Y_{\text{Exp}}$
$2_g^+ \rightarrow 0_g^+$	80.66	$1.15(9) \times 10^9$
$4_g^+ \rightarrow 2_g^+$	185.00	$1.41(11) \times 10^9$
$6_g^+ \rightarrow 4_g^+$	282.86	$1.55(14) \times 10^8$
$8_g^+ \rightarrow 6_g^+$	372.50	$7.32(87) \times 10^6$
$2_\gamma^+ \rightarrow 2_g^+$	807.50	$4.49(61) \times 10^7$
Doublet <sup>a</sup>	888.16 + 882.28	$5.49(78) \times 10^7$
$4_\gamma^+ \rightarrow 4_g^+$	795.33	$1.37(19) \times 10^7$
$4_\gamma^+ \rightarrow 2_g^+$	980.34	$7.31(131) \times 10^6$

<sup>a</sup> This peak is an unresolved doublet, comprising both the 888 keV  $2_\gamma^+ \rightarrow 0_g^+$  and 882 keV  $3_\gamma^+ \rightarrow 2_g^+$  transitions.

minimisation, Gosia refines the reduced matrix elements  $\langle I_f || E\lambda || I_i \rangle$  so that the simulated  $\gamma$ -ray yields reproduce experimental results. This procedure provides a semi-model-independent means of determining transition strengths, while also offering a direct route to theoretical comparisons through extracted  $B(E\lambda)$  values.

For  $^{162}\text{Dy}$ , the partial level scheme shown in Fig. 1 was defined in Gosia, incorporating all experimentally observed states, along with additional higher-lying ‘‘buffer’’ states from the ENSDF database [9], to ensure correct feeding pathways were available during the fit. A starting basis for the transition matrix was determined using the generalised collective model (GCM) code, which provides  $B(E2)$  transition strengths and quadrupole moments [17].  $M1$  transitions were also defined, according to literature mixing ratios.

Experimental  $\gamma$ -ray yields, corrected for efficiency and angular correlation effects (see Table 1), were input separately for each photodiode. Branching ratios and mixing ratios as reported by ENSDF were included as constrained parameters. Internal conversion coefficients were interpolated from the BRIC database [18].

The fitting proceeds through minimisation of the global  $\chi^2$  function. Since the  $\chi^2$  surface is often highly multidimensional and non-linear, the fitting can converge on local minima. One common cause of such minima is the sign (or phase) of the matrix elements, which determines whether interference between multiple excitation pathways is constructive or destructive. Since the minimisation algorithm cannot cross through  $\langle I_f || E\lambda || I_i \rangle = 0$ , phase reversals must be applied manually.

This process is still ongoing, however, preliminary results accurately reproduce experimental yields as well as literature constraints. Reduced matrix elements corresponding to observed transitions as well as quadrupole moments for the yrast- and single- $\gamma$ -band states observed show a strong sensitivity to the experimental data, allowing for precise measurements that agree with literature results within their uncertainties. Additionally, strong transitions from all

three possible two-phonon states to the  $K^\pi = 2^+$  single- $\gamma$  band are suggested. The sensitivity of the Gosia minimisation to these transitions, which were not directly observed, is still questioned, yet the results appear promising at this stage. This experiment, with a low- $Z$  beam, will serve as the first step towards understanding the high-lying states. As discussed below, including data from other experiments planned with high- $Z$  beams in a full Gosia analysis will provide greater sensitivity to the two-phonon-candidates.

## 4 Direction of Future Investigations

While the investigation, as presented above, provides an accurate measurement of transitions between the yrast- and single- $\gamma$ -bands, for a more accurate assessment of two-phonon contributions, further investigations are required. In particular, a higher- $Z$  beam, such as  $^{32}\text{S}$  or  $^{58}\text{Ni}$ , would enable stronger electromagnetic interactions and hence larger excitation cross sections for the possible multi-phonon states.

However, this approach presents significant experimental challenges. As the projectile charge and beam energy increase, so too does the complexity of the Coulomb-excitation process; the number of accessible states grows rapidly, necessitating a larger number of transition matrix elements to be included in the Gosia minimisation procedure. For this reason, the Coulomb-excitation investigation is done incrementally, with higher- $Z$  beams utilising the results of lower- $Z$  beam results to constrain the minimisation process.

Additionally, improved experimental selectivity and particle identification become essential for associating observed  $\gamma$ -ray transitions with specific reaction channels. The Mylar coating on the current particle-detectors also limit the available beam species, as higher- $Z$  beams fail to fully penetrate this layer at low energies.

### 4.1 New particle detection array for CAESAR

To extend the experimental reach of the HIAF, a new charged-particle detection array is currently under construction to fit inside the CAESAR target chamber, replacing the current silicon photodiode array. The system is based on the ‘‘phoswich’’ (phosphor sandwich) detection concept [19], in which two scintillator materials with distinct decay times are optically coupled and read out by a single silicon photomultiplier (SiPM). When a charged particle passes through the detector, it deposits different fractions of its energy in each layer depending on its mass, charge, and energy. The resulting composite pulse can be decomposed into its fast and slow components (as illustrated in Fig. 4), allowing for event-by-event discrimination between different particle species.

The new array will be designed to cover a broad angular range ( $\approx 65\%$  of  $4\pi$  coverage), with segmented modules providing position sensitivity and improved granularity compared to the current setup. Its deployment will mark

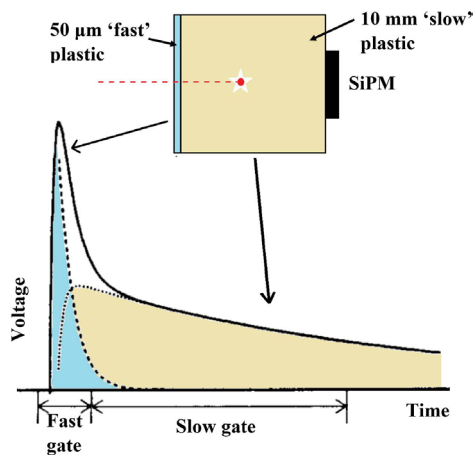


Figure 4: A diagram of a phoswich detector coupled to a silicon photomultiplier (SiPM), and an example signal produced (solid line). Portions of the signal corresponding to each part of the detector are highlighted. Adapted from Ref. [20].

a significant step forward for Coulomb-excitation studies at HIAF, enabling repeated investigations of  $^{162}\text{Dy}$  using higher-charge projectiles to probe multi-phonon configurations and test the limits of collective vibrational models in deformed nuclei.

## 5 Conclusion

In conclusion, the accurate measurement of two- $\gamma$ -phonon contributions in  $^{162}\text{Dy}$  is an ongoing research topic, with ramifications for the fundamental underpinnings of nuclear structure. Through Coulomb excitation with an  $^{16}\text{O}$  beam, the CAESAR array at HIAF was used to perform particle-gated  $\gamma$ -spectroscopy on a thin  $^{162}\text{Dy}$  target, with the aim of experimentally determining reduced transition matrix elements.

A number of intra-band transitions in the yrast band, as well as inter-band transitions between the single- $\gamma$  band and the yrast band, were observed. This paper presents an overview of the analysis methods used, as well as preliminary results, which suggest a set of matrix elements which accurately reproduce experimental  $\gamma$ -ray yields have been found, though more work to determine the sensitivity of the fit to several key matrix elements is required. The direction of future research, including a description of the phoswich detector system under development for increased Coulomb-excitation capabilities, was also presented.

## Acknowledgements

The authors wish to acknowledge the excellent work of the technical staff of the Department of Nuclear Physics and Accelerator Applications. T.N. Perissinotto, J.A. Woodside, and L.J. McKie acknowledge support of the Australian Government Research Training Program Scholarship. This material is based upon work supported by the

Australian Research Council Grant No. DP210101201 and the International Technology Center Pacific (ITC-PAC) under Contract No. FA520919PA138. The authors acknowledge the facilities, and the scientific and technical assistance provided by Heavy Ion Accelerators (HIA). HIA is supported by the Australian Government through the National Collaborative Research Infrastructure Strategy (NCRIS) program.

## References

- [1] A.N. Bohr et al., Collective and individual-particle aspects of nuclear structure, *Mat -fys Medd* **27**, 1 (1953). [10.1088/0031-8949/24/1B/001](https://doi.org/10.1088/0031-8949/24/1B/001)
- [2] H.G. Borner et al., Evidence for the existence of two-phonon collective excitations in deformed nuclei, *Phys. Rev. Lett.* **66**, 691 (1991). [10.1103/PhysRevLett.66.691](https://doi.org/10.1103/PhysRevLett.66.691)
- [3] T. Härtlein et al., Collective excitations built on the  $2^+$  state in  $^{168}\text{Er}$ , *The European Physical Journal A* **2**, 253 (1998). [10.1007/s100500050117](https://doi.org/10.1007/s100500050117)
- [4] C. Fahlander et al., Two-phonon  $\gamma$ -vibrational states in  $^{166}\text{Er}$ , *Physics Letters B* **388**, 475 (1996). [10.1016/S0370-2693\(96\)01203-8](https://doi.org/10.1016/S0370-2693(96)01203-8)
- [5] F. Corminboeuf et al.,  $K^\pi$  double-gamma vibration in  $^{164}\text{Dy}$ , *Physical Review C* **56**, R1201 (1997). [10.1103/PhysRevC.56.R1201](https://doi.org/10.1103/PhysRevC.56.R1201)
- [6] C.Y. Wu et al., Electromagnetic properties of the rotationally aligned band in  $^{162}\text{Dy}$ , *Physical Review C* **64**, 064317 (2001). [10.1103/PhysRevC.64.064317](https://doi.org/10.1103/PhysRevC.64.064317)
- [7] K.S. Krane et al., *Introductory nuclear physics* (Wiley, New York, 1987), ISBN 978-0-471-80553-3
- [8] A. Bohr et al., *Nuclear structure. 2: Nuclear deformations* (World Scientific, Singapore, 1998), ISBN 978-981-02-3980-0
- [9] N. Nica, *Nuclear Data Sheets for A=162*, *Nuclear Data Sheets* **195**, 39 (2024). [10.1016/j.nds.2024.04.001](https://doi.org/10.1016/j.nds.2024.04.001)
- [10] A. Aprahamian et al., Complete spectroscopy of the  $^{162}\text{Dy}$  nucleus, *Nuclear Physics A* **764**, 42 (2006). [10.1016/j.nuclphysa.2005.09.020](https://doi.org/10.1016/j.nuclphysa.2005.09.020)
- [11] A. Aprahamian et al., Lifetime measurements in  $^{162}\text{Dy}$ , *Physical Review C* **95**, 024329 (2017). [10.1103/PhysRevC.95.024329](https://doi.org/10.1103/PhysRevC.95.024329)
- [12] K. Heyde et al., Shape coexistence in atomic nuclei, *Reviews of Modern Physics* **83**, 1467 (2011). [10.1103/RevModPhys.83.1467](https://doi.org/10.1103/RevModPhys.83.1467)
- [13] D. Cline, Nuclear Shapes Studied by Coulomb Excitation, *Annual Review of Nuclear and Particle Science* **36**, 683 (1986). [10.1146/annurev.ns.36.120186.003343](https://doi.org/10.1146/annurev.ns.36.120186.003343)
- [14] T.R. Ophel et al., The 14UD pelletron accelerator at the Australian National University, *Nuclear Instruments and Methods* **122**, 227 (1974). [10.1016/0029-554X\(74\)90485-6](https://doi.org/10.1016/0029-554X(74)90485-6)
- [15] M. Reece et al., Coulomb excitation of  $^{124}\text{Te}$ : Emerging collectivity and persisting seniority structure in the  $6^+$  level, *Physical Review C* **112**, 034311 (2025). [10.1103/PhysRevC.112.034311](https://doi.org/10.1103/PhysRevC.112.034311)

- [16] D. Cline et al., GOSIA User Manual for Simulation and Analysis of Coulomb Excitation Experiments (2012).
- [17] D. Troltenier et al., in *Computational Nuclear Physics I: Nuclear Structure*, edited by K. Langanke et al. (Springer, Berlin, Heidelberg, 1991), pp. 105–128, ISBN 9783642763564, [https://doi.org/10.1007/978-3-642-76356-4\\_6](https://doi.org/10.1007/978-3-642-76356-4_6)
- [18] T. Kibédi et al., Evaluation of theoretical conversion coefficients using *BrIcc*, Nuclear Instruments and Methods in Physics Research Section A **589**, 202 (2008). [10.1016/j.nima.2008.02.051](https://doi.org/10.1016/j.nima.2008.02.051)
- [19] D.H. Wilkinson, The Phoswich—A Multiple Phosphor, Review of Scientific Instruments **23**, 414 (1952). [10.1063/1.1746324](https://doi.org/10.1063/1.1746324)
- [20] L. Wissink et al., Particle identification in phoswich detectors by signal width measurement, Nuclear Instruments and Methods in Physics Research Section A **397**, 472 (1997). [10.1016/S0168-9002\(97\)00715-8](https://doi.org/10.1016/S0168-9002(97)00715-8)